Precipitation Retrievals from Resolution-Matched GMI Brightness Temperatures

G. W. Petty and G. Shaughnessy
Atmospheric and Oceanic Sciences, University of Wisconsin-Madison

Overview

Petty (2013) and Petty and Li (2013a,b) demonstrated a new Bayesian retrieval methodology for surface rainfall estimation from resolution-matched TRMM Microwave Imager (TMI) data, using co-colocated Precipitation Radar (PR) rain rates as the calibration data source. Unique features of this algorithm include the following:

- A novel objective surface type classification based on "similarities" between the means and covariances of multichannel microwave TBs computed for each 1-deg. grid box.
- A novel dimensional reduction technique (Petty 2013) that improves the discrimination of precipitation against noisy backgrounds.
- A precomputed Bayesian lookup table that yields not only a mean surface rain rate but also a complete PDF of possible rain rates for any given TMI pixel.
- Validation of the algorithm against one year of independent PR data demonstrated roughly factor-of-two improvement in RMS error relative to the standard 2A12 rainfall product over virtually every surface type.

The above methodology has now been adapted to the GPM Microwave Imager (GMI) and applied to the first 1.7 years of GMI data (March 2014 – December 2015, using GPM Dual-frequency Precipitation Radar (DPR) Ku-band rain rates as the training data source.

An early attempt, presented last year (and using far less training data), did not quite achieve the performance previously demonstrated for TRMM. We attributed the degraded error statistics to the following factors:

- Resolution-matched TBs were not available for GMI, so spatial gradients introduced considerable noise into the retrievals, in contrast to the case for the earlier TMI implementation.
- Variations in land surfaces are considerable greater for the GPM owing to its coverage of a much wider range of latitudes (roughly 68S–68N, as compared to 38S–38N for TRMM). Ice and snow are major factors.

We therefore undertook the following tasks:

1. Derivation of coefficients for (de)convolving all GMI channels to a common EFOV similar to that of the 18.7 GHz channels (Petty and Bennartz 2015, see **Fig. 1** and **Table 1**).
2. Derivation of a new surface classification map using a larger number (12) of distinct surface types (**Fig. 2**).
3. Creation of a matchup database from resolution matched GMI TBs and DPR (Ku) rain rates.
4. Objective derivation of dimensional reduction coefficients and a new Bayesian data base (in lookup table form) comprising one-half of the available 1.7 years of matchups.
5. Initial validation against the independent half of the data from the same period (**Figs. 3 –5**).

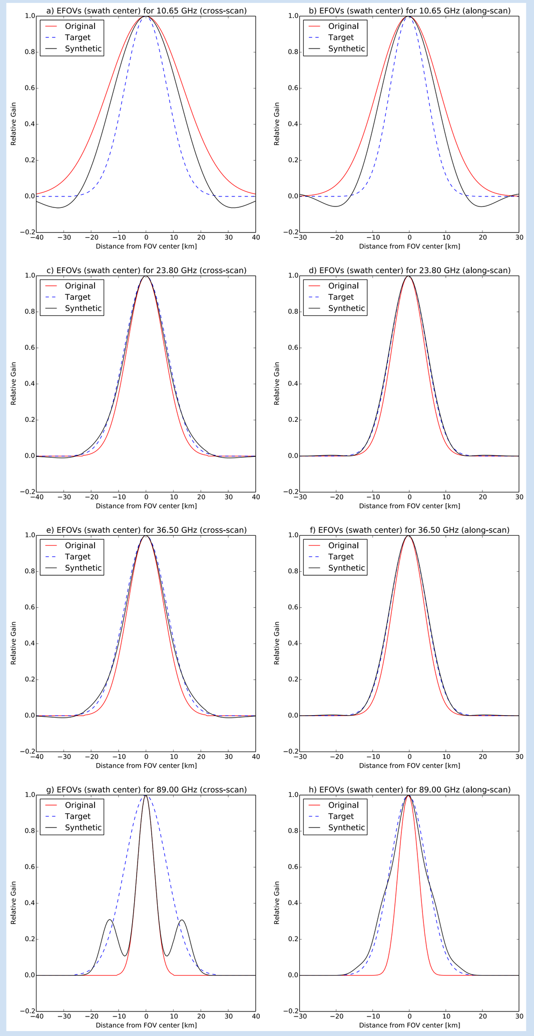

Figure 1: Along- and across-scan effective fields-of-view (EFOVs) for GMI channels from 10.65 to 89 GHz, before and after (de)convolution according to the method of Petty and Bennartz (2016)

Table 1 Comparison of native and resolution-matched EFOV 3 dB widths [km].

Frequency	Cross-Scan		Along-Scan	
	Native	Matched	Native	Matched
10.65	32.1	26.5	19.8	16.5
18.70	18.1	18.1	11.8	11.8
23.80	16.0	18.0	10.6	11.8
36.50	15.6	18.0	10.3	11.8
89.00	7.2	(7.2)	6.3	11.8

Table 1: The numerical beamwidths corresponding to the results in Fig. 1.

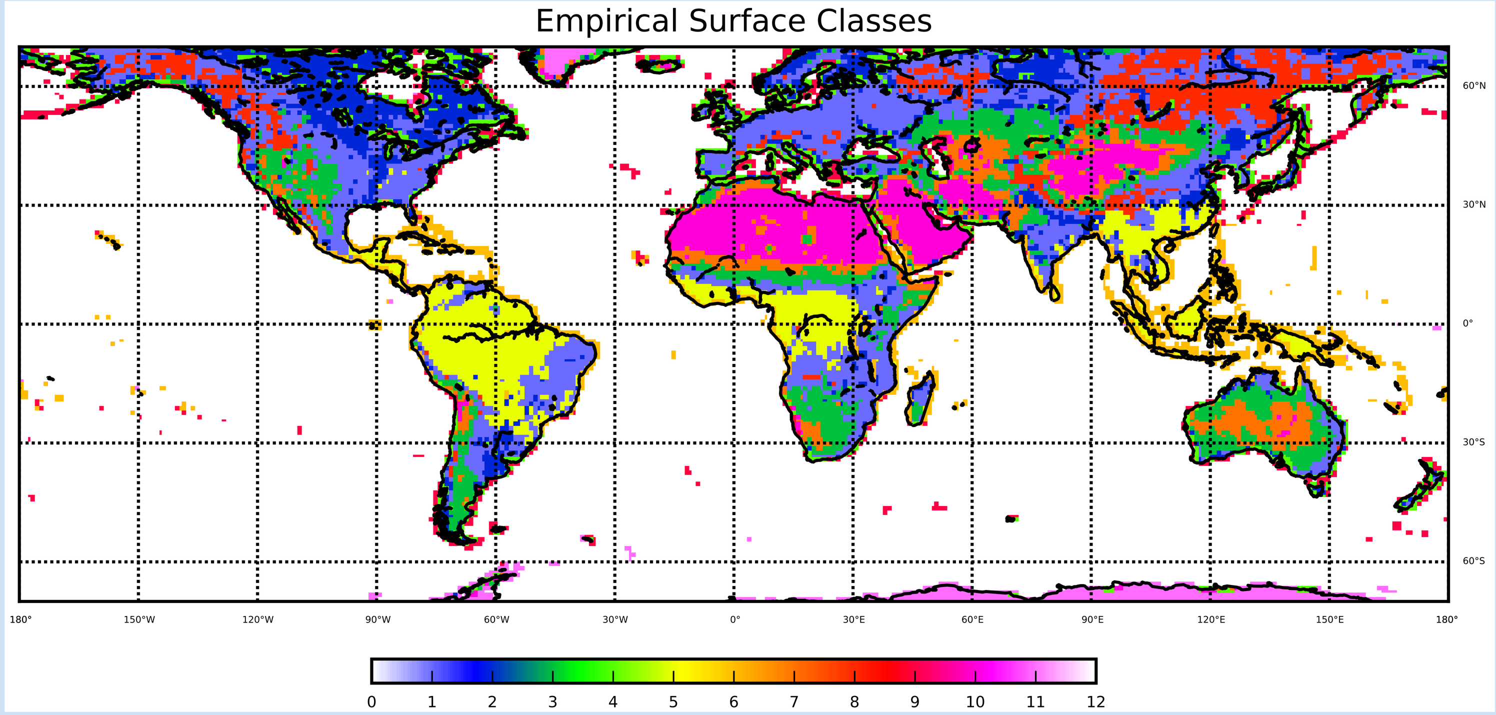

Figure 2: Map of the 12 objectively determined land surface classes. GMI data falling into these classes were further subdivided according to whether Tskin was above or below 275 K, an indication as to whether surface snow or ice needed to be considered.

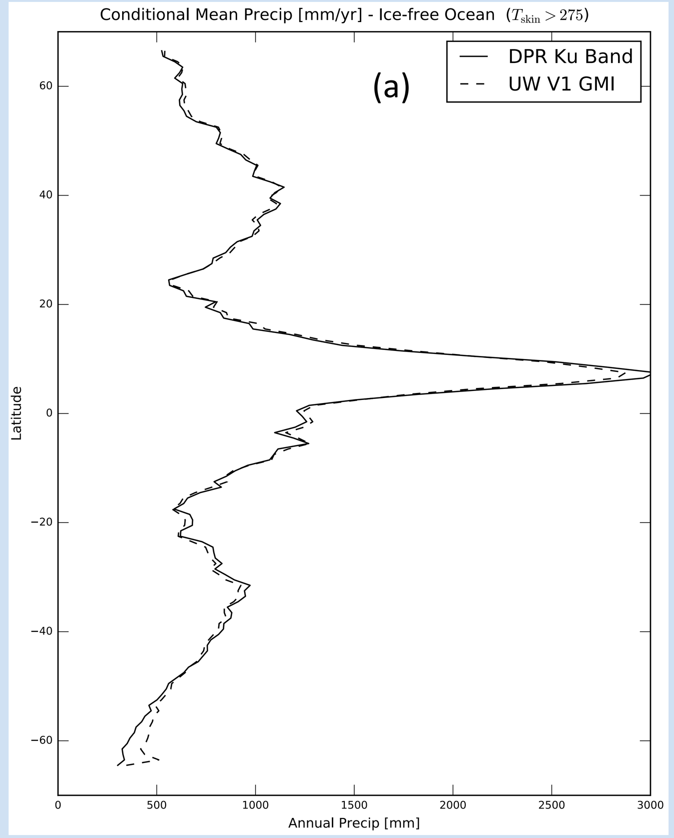

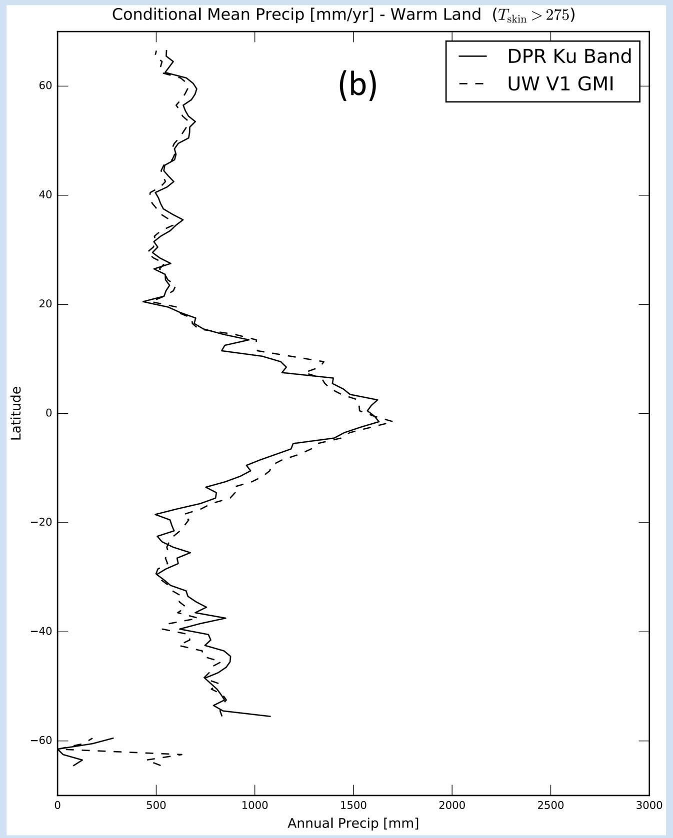

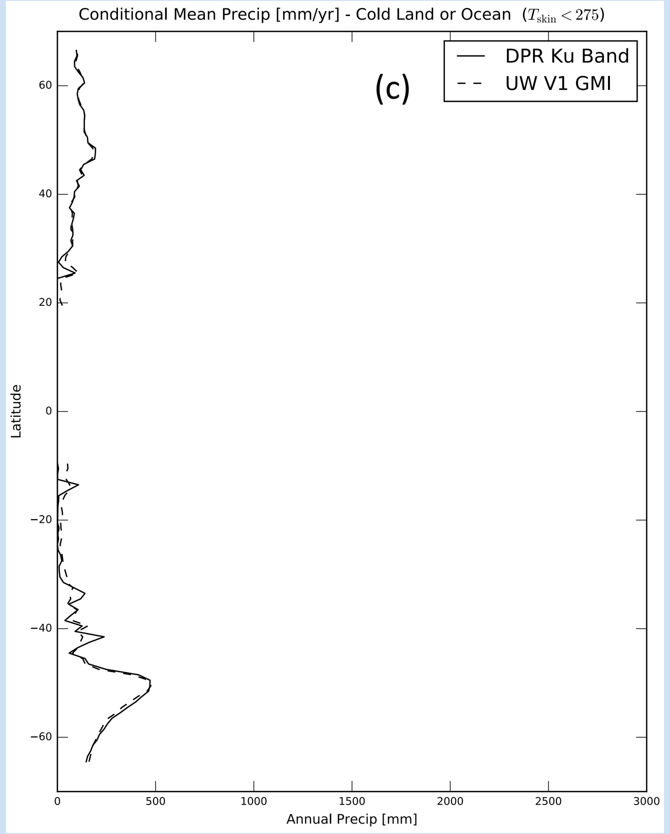

Figure 3: Latitudinal profiles of rainfall from GMI compared with independent DPR Ku-band rainfall estimates for three different surface types. a) Ice free ocean. b) Ice free land. c) Cold land and ocean (possible ice).

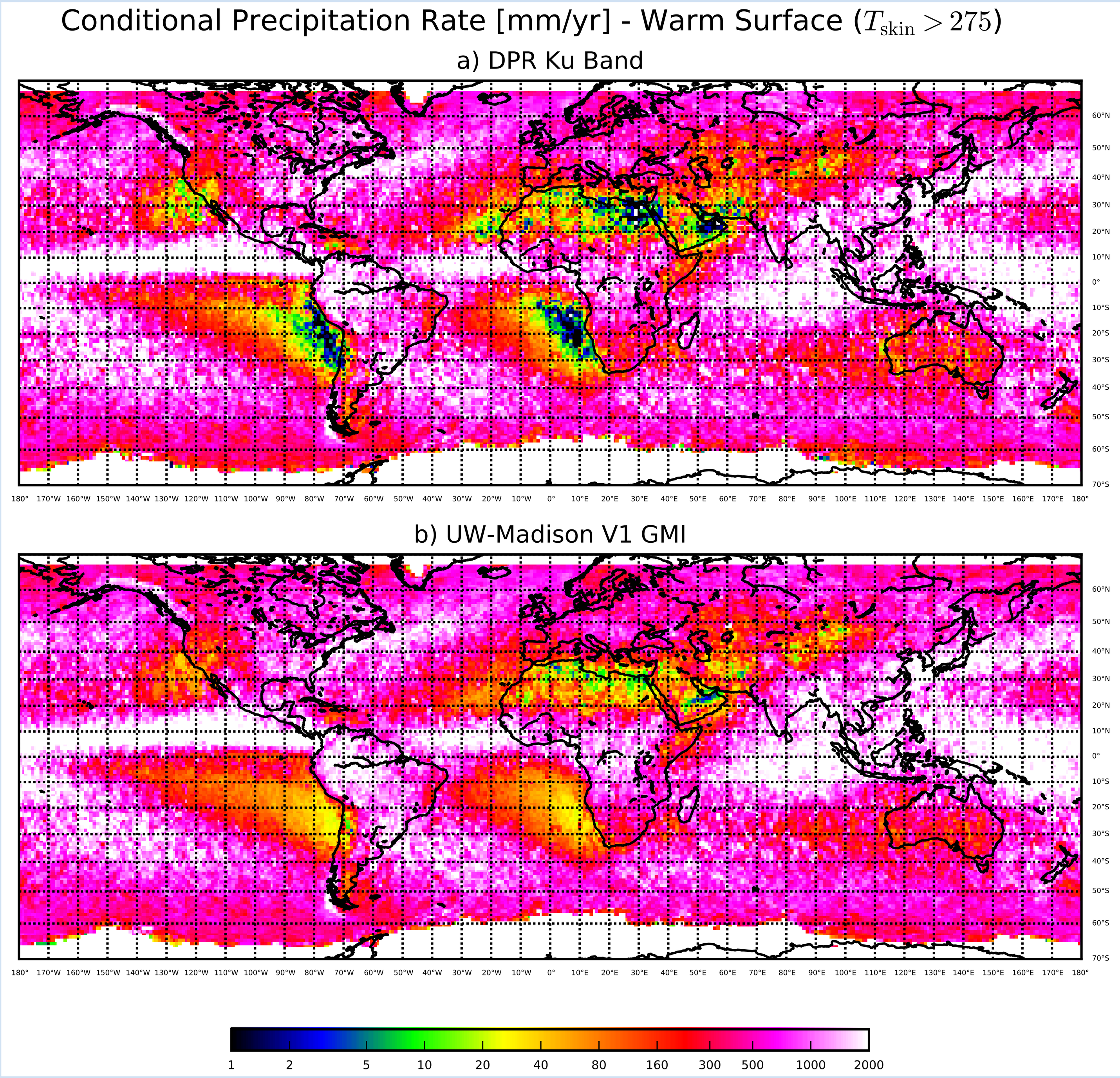

Figure 4: Comparison of GMI-derived precipitation with DPR (Ku-band) derived precipitation, conditioned on surface skin temperatures warmer than 275K

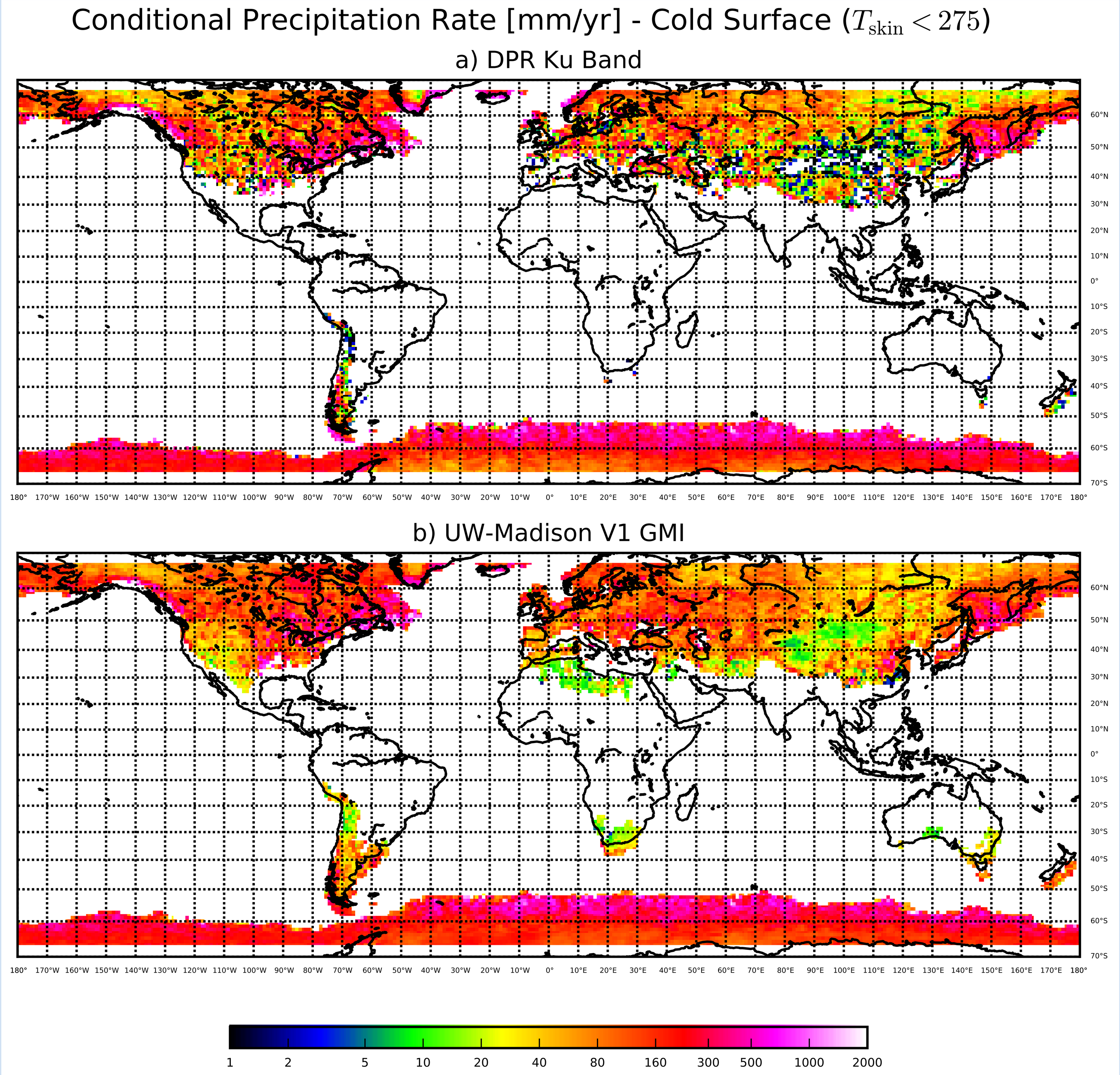

Figure 5: Comparison of GMI-derived precipitation with DPR (Ku-band) derived precipitation, conditioned on surface skin temperatures colder than 275K and thus possibly affected by snow or ice.

References

Petty, G. W., 2013: Dimensionality reduction in Bayesian estimation algorithms. *Atmos. Meas. Tech., 6, 2267-2276.*

Petty, G. W. and R. Bennartz, 2016 Field-of-view characteristics and resolution matching for the Global Precipitation Measurement (GPM) Microwave Imager (GMI), *Atmos. Meas. Tech. Discuss.*, in review.

Petty, G. W., and K. Li, 2013a: Improved Passive Microwave Retrievals of Rain Rate over Land and Ocean. Part I: Algorithm Description. *J. Atmos. Ocean. Tech.*, **30**, 2493-2508.

Petty, G.W., and K. Li, 2013b: Improved passive microwave retrievals of rain rate over land and ocean. Part II: Validation and intercomparison. *J. Atmos. Ocean. Tech.*, **30**, 2509-2526.

Acknowledgements

This work was supported by the NASA PMM project via NASA Grants NNX13AG49G and NNX16AF70G.